Analytical and Experimental Investigation of a Magnetic Radial Passive Damper

G. GENTA,* C. DELPRETE,* A. TONOLI,* E. RAVA** AND L. MAZZOCCHETTI**

ABSTRACT

Passive radial magnetic bearings are well suited for magnetic bearing systems both for one active-axis type and for hybrid solutions in which a passive radial magnetic bearing works together with a conventional rolling element bearing for stability. In both cases, and particularly in the first one, the damping of the system is a critical factor to achieve the required performance, as the very low stiffness and damping characterizing the radial passive suspension can cause severe dynamic problems. The possible existence of instability regions within the supercritical working range must be avoided by adding adequate damping elements.
An eddy-current passive radial damper with a simple geometrical configuration is studied firstly using analytical techniques of different complexity. The distribution of the magnetic flux density in the conductor is obtained through FEM numerical modeling. The results obtained through the combined analytical and numerical technique are found in very good agreement with those obtained through experimental testing.
The passive radial damper here studied can have applications beyond the field of passive radial magnetic bearing as it allows to raise the threshold of instability of a rotor of any type with the addition of a simple and basically low-cost device. If the magnetic field is supplied by an electromagnet instead of a permanent magnet, the possibility of supplying a damping which is both controllable and well predictable is an attractive feature added to its simplicity and low cost.

INTRODUCTION

The rotor suspension system of any rotating machine must include an adequate amount of damping in order to insure a safe and stable operation. This is particularly true for machines operating in the supercritical range, where the damping of the nonrotating parts of the system performs the two tasks of allowing the crossing of the critical speeds without severe vibrations and raising the threshold of instability above the working range. In the case of one active-axis magnetic suspensions, in which the radial magnetic bearings are of the passive type, this need is particularly strong as the damping of the radial bearings is low and a purposely designed damper must be incorporated into the system [1], [2].
It is well known that the effects of damping on the dynamic behaviour of a rotating machine is much different depending whether the damping elements are stationary or rotating at the spin speed [3]. While "nonrotating" damping has always a stabilizing effect on the whirl motion of the machine, "rotating" damping is generally speaking stabilizing for all whirl motions occurring at a frequency higher than the rotational speed and unstabilizing in other cases. Eddy-current

* Dipartimento di Meccanica, Politecnico di Torino, C.so Duca degli Abruzzi, 24, 10129 Torino, Italy
** Elettrorava S.p.A., v. Don Sapino, 176, 10040 Savonera Torino, Italy

dampers are no exception to this general rule: the damping element, in this case the conducting material in which energy is dissipated owing to the eddy currents, must be stationary if the device has to have a "stabilizing" effect in the supercritical range.
During the development of the two turbomolecular pumps described in [4] the need for a more detailed study in this area was felt. While in the first of the two machines there described the rolling element bearing used in the hybrid suspension layout provided enough damping to insure a very stable operation in the supercritical range, the second layout, based on a one active-axis suspension, showed the need of a more efficient damping system.
Several possible solutions were considered. A first obvious choice is the use of an active magnetic damper, e.g. as the one described in [5]. However the very choice of a passive radial bearing system was motivated by the need of keeping the system as simple as possible in order to reduce costs and the use of an active damper was felt as conflicting with this choice. Another possible option is the use of a mechanical damper, simply by incorporating one of the radial passive bearings in a damped support, perhaps based on the use of an adequate elastomeric material. Also this solution, which was used in existing applications and described in the literature [6], was discarded on the grounds of the added complexity and, even more, of the added bulk of the system.
The chosen configuration was a passive eddy-current damper, consisting of a stationary copper disc connected to the stator of the machine and a rotating magnetic circuit with a permanent magnet polarized axially. This configuration allows to introduce the required damping into the system without adding much to the cost, the complexity and the bulk of the machine. The design of this device is however not straightforward, as there exist no simple formulae for the prediction of its performance, although eddy-current dampers have been the subject of several papers, particularly those by K. Nagaya ([7] to [10]). Apart from the derivation of a very simple formula linking the damping forces with the magnetic field, which can be used in order to understand the type of the dependence of the damping forces from the relevant parameters, the problem was solved firstly by following the analytical approach suggested by Nagaya in [9] and adapting it to the relevant geometrical configuration. As the key for a good evaluation of the damping force is the correct simulation of the magnetic field in the conducting material, a finite element model of the magnetic circuit was built and the results so obtained were incorporated into the analytical approach. Extensive experimental testing confirmed the results obtained through the analytical and numerical models, allowing to use with confidence the results obtained.
The eddy-current dampers here studied can have fields of application well beyond that of one active-axis magnetic suspensions: their characteristics of supplying a reliable and easily predictable damping force, which can as well be controllable if the magnetic field is provided by an electromagnet, make them very interesting also for applications to a wider class of machines.
A different class of eddy-current passive device for rotor suspension are eddy-current bearings (e.g. [11]); however the present study is not intended to apply to them.

ANALYSIS

FIRST APPROXIMATION APPROACH

The relative motion between a conductor and a magnetic field generates eddy currents that interact with the magnetic field giving a force in a direction opposite to the relative motion. In order to obtain a first approximation formula to evaluate the force acting on the damper sketched in Figure 1 (in which the magnetic circuit is a part of the rotor while the disc of conducting material is stationary) and the related damping coefficient, the Maxwell's equations can be simplified following the assumptions that the relative velocity is small, leading to negligible variations in time of the eddy currents, and the resistance of the current paths outside the region of the conductor intersected by the magnetic field is vanishingly small.
The equations describing the electric field in the conductor are therefore

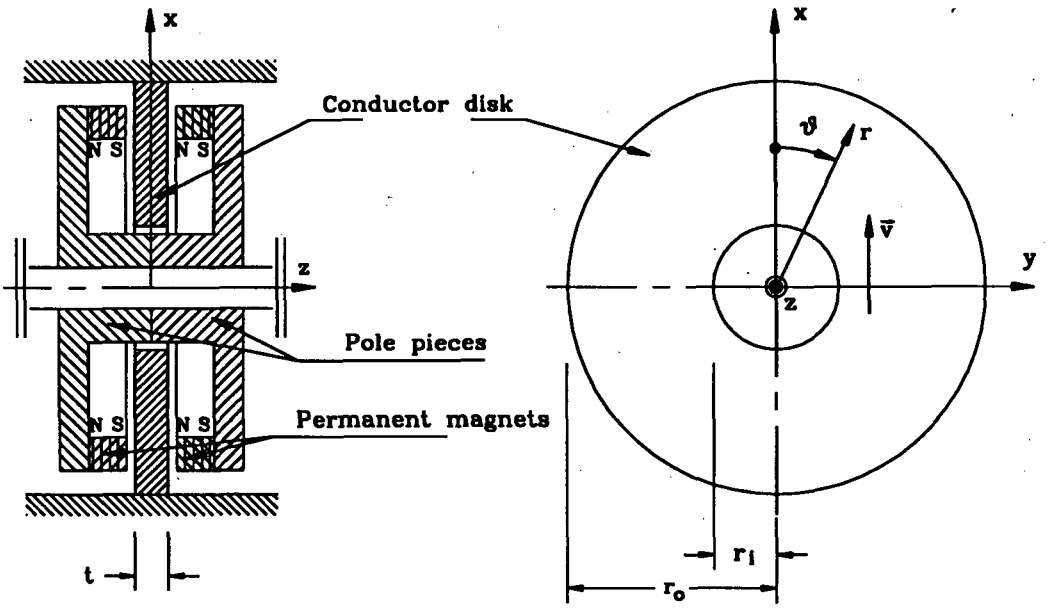

Figure 1. Geometrical layout of the eddy-current damper.

$$\vec{E}=\vec{v}\times\vec{B} \quad ; \quad \vec{J}=\frac{\vec{E}}{\rho} \quad ; \quad \vec{F}_V=\vec{J}\times\vec{B} \quad \text{and then} \quad \vec{F}_V=\frac{(\vec{v}\times\vec{B})\times\vec{B}}{\rho} \quad . \tag{1}$$

$\vec{E}, \vec{B}, \vec{J}, \vec{v}$ and ρ are respectively the electric field, the magnetic flux density, the eddy current density, the relative velocity and the conductor resistivity; $\vec{F}_V$ is the magnetic force density. Considering that $\vec{B}$ is perpendicular both to $\vec{v}$ and to the conductor surface and constant through the conductor thickness, the total force acting on the conductor is

$$\vec{F}=\int_V \vec{F}_V dV=\frac{-\vec{v}t}{\rho}\int_{A_f} B^2 dA \tag{2}$$

where A_f is the area of the conductor of thickness t intersected by the magnetic field. Equation (2) shows that the eddy-current damper can be modelled as a linear viscous damper, as it provides a force proportional to the velocity $\vec{v}$ and opposing it. By indicating with $\overline{B^2}$ the average value of the square of the magnetic flux density in the conductor and as $V = tA_f$ the relevant volume of the conductor, the viscous damping coefficient takes the value

$$c = V\overline{B^2}/\rho \quad . \tag{3}$$

The damping coefficient is then proportional to the volume of the conductor intersected by the magnetic field and to the average of the square of the magnetic flux density and inversely proportional to the resistivity of the conductor. Equation (3) gives an over-estimate of the actual damping because the resistance of the current paths in the outer region of the conductor has been neglected; for the same reason in equation (3) there are no parameters related to the shape of the conductor.

SECOND APPROXIMATION APPROACH

The aim is to take into account the dissipation of the current paths outside the region of the conductor intersected by the magnetic field. The method employed is that proposed by K. Nagaya [9]; in the present paper this method has been particularized in order to study a circular conductor with an axial circular hole. Owing to the axial symmetry of the device, the conductor can be subdivided into a number of annular elements as shown in Figure 2. Making the same low relative velocity assumption of the first approximation approach, the equations describing the eddy current distribution induced in the conductor are

$$\nabla^2\phi = \nabla \cdot \vec{E} \quad ; \qquad \vec{E} = \vec{v} \times \vec{B} \quad ; \qquad \vec{J} = \frac{(\vec{E} - \nabla\phi)}{\rho} \quad , \tag{4}$$

from which it follows $\nabla^2\phi = \nabla \cdot (\vec{v} \times \vec{B})$, or, using the cylindrical frame r, θ, z fixed with respect to the magnetic field of Figure 1,

$$\left(\frac{\partial^2}{\partial r^2} + \frac{1}{r}\frac{\partial}{\partial r} + \frac{1}{r^2}\frac{\partial^2}{\partial \theta^2} \right) \psi = \sin\theta \frac{\partial q}{\partial r} + \frac{\cos\theta}{r}\frac{\partial q}{\partial \theta} = f(r, \theta) \quad . \tag{5}$$

$\psi = \phi / v$; q is the discretized magnetic flux density, $q = \sum_{k=1}^{K} [u(r - r_{k-1}) - u(r - r_k)] B_k$ and $u(r - r_k)$ is the unit step function.

Expanding the unknown potential ψ and the known function $f(r, \theta)$ in Fourier series, following the same scheme of solution adopted by Nagaya in [9] and taking into account the symmetry of the problem, the following solution can be found

$$\begin{aligned} \psi = & \sum_{n=1}^{\infty} (\overline{A}_n r^n + \overline{B}_n r^{-n}) \sin(n\theta) + \\ & + \sum_{k=1}^{K} \left\{ \frac{r}{2} [u(r - r_{k-1}) - u(r - r_k)] - \frac{1}{2r} [r_{k-1}^2 u(r - r_{k-1}) - r_k^2 u(r - r_k)] \right\} B_k \sin\theta \quad . \end{aligned} \tag{6}$$

The eddy currents must be parallel to the inner and outer edges of the conductor; this condition can be written in terms of potential as

$$\frac{\partial \psi}{\partial r} = 0 \qquad r = r_i, r_o \quad . \tag{7}$$

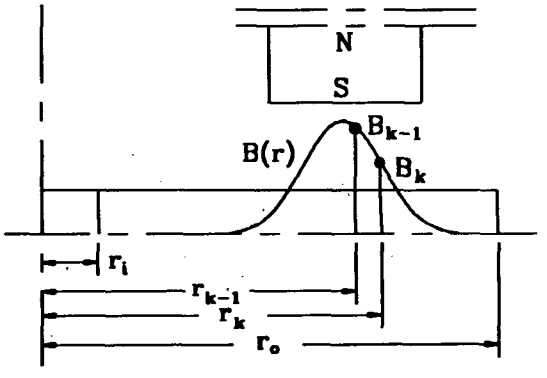

Figure 2. Distribution of the magnetic flux density in the conductor.

Substituting equation (6) into equation (7), the following expressions of the unknown coefficients can be obtained

$$\overline{A}_1 = \sum_{k=1}^{K} \frac{r_k^2 - r_{k-1}^2}{2(r_o^2 - r_i^2)} B_k \quad , \qquad \overline{B}_1 = \sum_{k=1}^{K} r_i^2 \frac{r_k^2 - r_{k-1}^2}{2(r_o^2 - r_i^2)} B_k \quad , \qquad \overline{A}_j = \overline{B}_j = 0 \quad \text{for} \quad j > 1 \quad , \tag{8}$$

which allows to compute the potential ψ.

Only the component of the eddy current density $\vec{J}$ in y direction contributes to the damping force; it can be evaluated by the last of the equations (4) rewritten as

$$J_y = \frac{\nu}{\rho}[-(\nabla\psi)_y + q] \quad . \tag{9}$$

The Lorentz force for the small volume $dV = t r dr d\theta$ is

$$(dF_x)_k = B_k (J_y)_k t r dr d\theta \quad . \tag{10}$$

Integrating over the conductor region intersected by the magnetic field it follows

$$F_x = -\nu \frac{\pi(r_o^2 - r_i^2)t}{\rho} \sum_{k=1}^{K} B_k \frac{r_k^2 - r_{k-1}^2}{r_o^2 - r_i^2} \left(\frac{B_k}{2} - \overline{A}_1 \right) \quad . \tag{11}$$

The damping force is also in this case proportional to the velocity and the device is equivalent to a linear viscous damper with damping coefficient

$$c = \frac{\pi(r_o^2 - r_i^2)t}{\rho} \sum_{k=1}^{K} B_k \frac{r_k^2 - r_{k-1}^2}{r_o^2 - r_i^2} \left(\frac{B_k}{2} - \overline{A}_1 \right) = \frac{t}{2\rho} \left(\frac{-\Phi^2}{A} + \sum_{k=1}^{K} B_k \Phi_k \right) \quad , \tag{12}$$

where the magnetic flux is $\Phi = \int_A \vec{B} \cdot \overrightarrow{dA}$ and A is the area of the whole conductor $A = \pi(r_o^2 - r_i^2)$. Equation (12) has been obtained from an exact solution of the field equations (4); therefore the value of the damping coefficient c holds whenever the assumptions on which the equations (4) are based are acceptable.

EVALUATION OF THE MAGNETIC FIELD DISTRIBUTION

The knowledge of the magnetic flux density distribution in the conducting material, i.e. the values of B_k in equation (12), is very important in order to compute the damping force produced by the device. The values of B_k and the extension of the conductor region intersected by the magnetic field must be obtained with good approximation in order to obtain reliable results. As the analytical evaluation for the geometry here considered is quite complicated, for design purposes two ways can be suggested: experimental measuring or numerical simulation. At the design stage the second approach can be followed without problems as it does not involve complex numerical simulation. A nonlinear computation can be needed to take into account the possible saturation of the material but an axi-symmetrical model can be used in the case of the geometrical configuration of the magnetic circuit of Figure 1.

Once that the numerical simulation, e.g. performed using the finite element method (FEM), has been completed, equations (3) or (12) yield directly the damping coefficient. Alternatively, the computation can be completely performed using a suitable FEM code to compute the eddy current distribution and hence the damping force. This last approach requires a tri-dimensional model of the magnetic circuit and conductor disc in an off-centre position and is far more exacting for what the computer time and hardware size are concerned. In the opinion of the authors it gives also a smaller insight on the dependence of the results on the relevant parameters, if not at the cost of a very long parametric study. However, this last approach does not rely on the assumption of small relative velocity $\vec{v}$ and can be needed when the values of $\vec{v}$ are sufficiently high.
Note that the assumption of small velocity allows to obtain a formulation of the eddy-current damper equivalent to a linear viscous device and is surely applicable to the analysis in the small for the study of the stability of the whirl motion. This situation is the typical one regarding linearized theories which are common in the study of all damping devices.

EXPERIMENTAL VALIDATION

In order to verify the applicability of the results obtained in the preceding section to actual cases, an experimental validation of the analytical formulae, with the values of the magnetic field distribution obtained through FEM modelling, was devised. In order to overcome the difficulties linked with the experimental measurement of the damping force obtained from the geometrical configuration shown in Figure 1 when performing a general whirling motion, some modifications of the device were introduced. This does not detract from the applicability of the conclusions to actual cases, as the mentioned changes where accounted for also in the analytical and numerical models.
Firstly, the magnetic field was provided by an electromagnet instead of a permanent magnet. This allowed to control easily the magnetic field and to investigate the dependence of the damping force from it in a straightforward way, without the need of using different permanent magnets. Instead of using a stationary damping element in a field generated by rotating magnets, the damping element was rotated while the magnets were fixed to the stator of the machine. While this layout is obviously useless for the practical purpose of damping whirl motions, it has two notable advantages from the experimental viewpoint: it avoids the complexity of delivering the required current to a rotating coil and simplifies the measuring of the damping force. The system used for the experimental testing is sketched in Figure 3.
Consider a rotating system operating at constant speed in steady-state condition, without performing any whirling motion. The equation yielding the deflected shape of a discretized model can be written in the form

$$([K] - i\omega[C_r])\{q\} = \{F\} \tag{13}$$

where $\{q\}$ is a vector of complex co-ordinates, which in case of steady-state rotation is constant in time, $\{F\}$ is a vector of forces applied to the system and $[K]$ and $[C_r]$ are respectively the stiffness and rotating viscous damping matrices [12].
If the rotor of Figure 3 is displaced of distance d in x direction, with respect to the stator, while rotating at the angular velocity ω, and assuming that the rotating damping due to the eddy currents is of the viscous type, the stator experiences a static force in y direction whose modulus, computed through equation (13), is

$$|F_y| = \omega d c_r \quad , \tag{14}$$

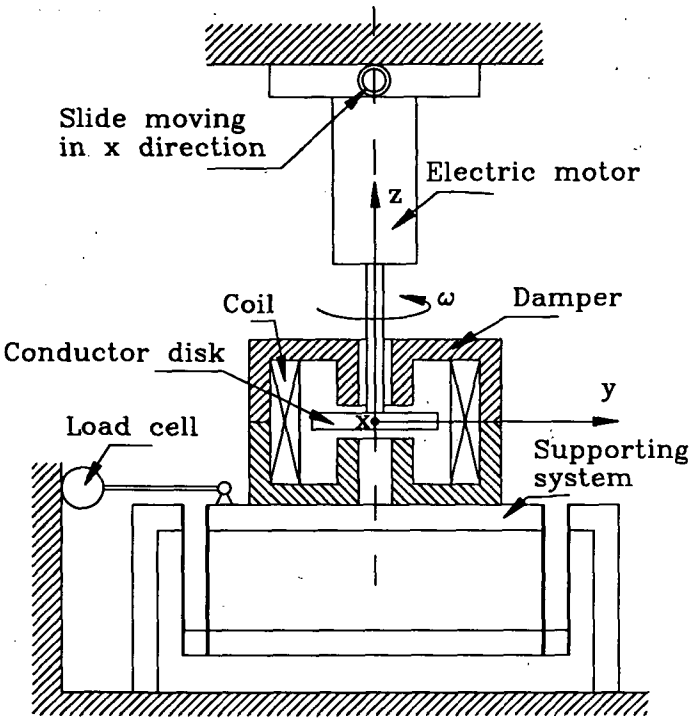

Figure 3. Geometrical layout of the device used for experimental testing.

which can be very easily measured. Note that small displacements in y direction of the rotor do not produce any force in the same direction which can influence the measurement, unless their amplitude is so large to invalidate the assumption of linearity of the whole device. This way of measuring the damping is equivalent to the usual way of measuring the internal damping of materials from the lateral inflection during a rotating bending test.

The drive motor is mounted on a micrometric slide in order to control very accurately distance d while the stator is mounted on a force-measuring device consisting in a suspended table and restrained by a load cell.

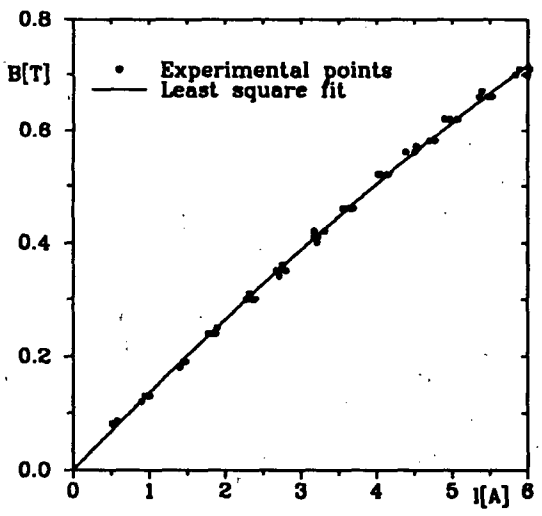

Figure 4. Magnetic flux density versus coil current. Experimental points and parabolic least-square interpolation.

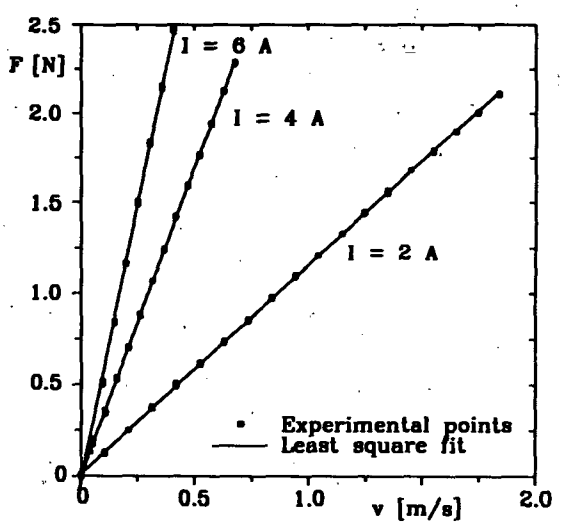

Figure 5. Experimental force-velocity dependence at $\omega = 10000$ rpm.

TABLE I - VALUES OF THE DAMPING COEFFICIENT c IN Ns/m AT DIFFERENT SPEEDS FOR DIFFERENT VALUES OF THE CURRENT. VALUES OBTAINED THROUGH EXPERIMENTS AND EQUATIONS (3) AND (12).

ω [rpm]	7500	10000	12500	15000	eq.(3)	eq.(12)
$I = 2$ A	1.144	1.253	1.162	0.769	6.305	1.180
$I = 4$ A	3.939	3.703	3.651	2.888	26.759	3.583
$I = 6$ A	7.326	6.636	5.878	5.262	48.262	6.471

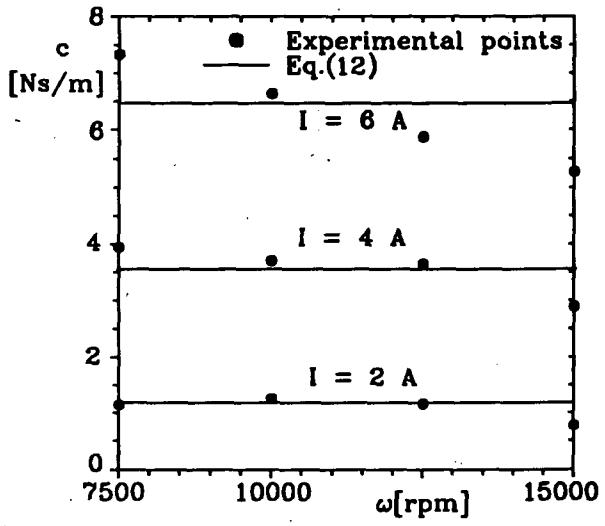

Figure 6. Damping coefficient versus angular speed. Experimental results compared with those obtained through equation (12).

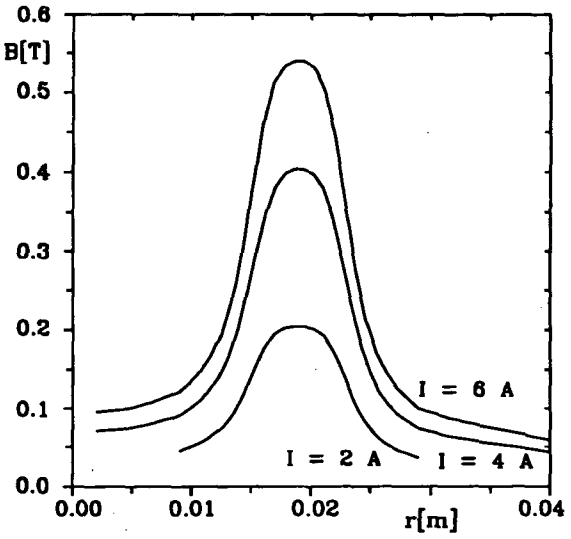

Figure 7. FEM Magnetic flux density distributions.

This type of suspension was chosen in order to support the relatively heavy weight of the stator, which includes the coil, without causing any friction influencing the force results. Its kinematical design prevents any vertical motion of the table linked with its horizontal motion: the weight of the device does not load directly the load cell in any position of the table. The stiffness of the supporting system and that of the load cell were measured, obtaining $k_s = 3.511$ N/mm and $k_c = 30.534$ N/mm respectively.

Some preliminary tests aimed to characterize the coil were firstly run. The absolute value of the magnetic flux density $\vec{B}$ was measured at different values of the coil current using a gaussmeter fixed to one of the polar expansions; the results of the tests are reported if Figure 4. The slope of the parabolic least-square interpolation is in the origin 0.139 T/A while the same value computed from the characteristics of the coil is 0.135 T/A.

All force measurements were conducted by imposing a given current to the coil and running the rotor at a preset speed. A "centred" position in which the force on the load cell was zero was found by monitoring the force output while moving the micrometric slide. The axis of the rotor was then displaced from this centred position in steps of 0.1 or 0.05 mm depending on the value of the coil current, reading the value of the force at each step. Various test runs were performed for different values of the spin speed and the whole procedure was repeated for different values of the coil current.

The results obtained at an angular speed $\omega = 10000$ rpm and at a coil current $I = 2, 4, 6$ A are reported in Figure 5 together with the linear least-square interpolations. The linear dependence of the damping force on the velocity is clear, the assumption that the eddy-current device behaves as a linear viscous damper is so confirmed.

Since the supporting system and the load cell behave as two springs "in parallel", the actual damping coefficient can be obtained by multiplying the slopes of the straight lines of Figure 5 by a factor $(1 + k_s/k_c)$. The actual values of the damping coefficient so obtained are summarized in Table I. The same data are also reported in Figure 6.
Some differences between the measured behaviour of the device and the expected linear behaviour are visible in Figure 6. While the damping coefficient at $I = 2$ A is practically independent from the angular speed (as the linear theory predicts), the effect of the speed is not negligible at $I = 4$ A and even more at $I = 6$ A. A possible explanation of this effect can be linked with the heating of the conductor that, increasing the resistivity of the material, lowers the damping coefficient. This effect is now being evaluated and further experimental work is needed.
The dependence of the damping coefficient on the coil current, particularly for high values of the latter, is not exactly quadratic as could be expected, but this can be easily explained with the nonlinear nature of the permeability of the material (see also Figure 4).

COMPARISON BETWEEN COMPUTED AND MEASURED RESULTS

An axi-simmetrical FEM model of the magnetic circuit was built in order to compute the magnetic flux density distribution in the conductor. The model consists of 1584 3D multi-field solid eight-node elements and the solution was performed using the ANSYS 4.4A code (magnetostatic solution) running on a VAXstation 2000. The results obtained for the three values of the coil current considered in the experimental tests are reported in Figure 7.
From these results the values of the damping coefficient computed using equations (3) and (12) are reported in the last two columns of Table I. The results obtained from equation (12) are also reported in Figure 6.

CONCLUSIONS

An eddy-current damper of basic geometric shape to be used for stabilizing the whirl motion of rotors, particularly in the case of one active-axis magnetic suspension, has been studied in detail.
The analytical study confirmed that the device produces a damping force which is proportional to the velocity and hence can be assimilated to a linear viscous damper. This conclusion has been drawn under the assumption that the relative velocity is enough small.
The main difficulty of the analytical approach is that of predicting the distribution of the magnetic flux density in the conductor. This part of the computation has been dealt with through numerical modeling, using a standard FEM code.
An experimental facility has been constructed and a series of tests has been performed on a simple device which simulates well the behaviour of the damper while allowing simple and reliable measuring of the damping force. The experimental results allowed to ascertain that the damping force is very closely proportional to the relative velocity in each test conducted at constant speed of the experimental device. However, in tests conducted at different speeds, some dependence of the damping coefficient from the angular velocity has been recorded. Further research on this topic, which would introduce, if confirmed, a certain nonlinearity in the behaviour of the system, is planned.
While the agreement between the results obtained through the first approximation approach (equation 3) and the experimental results is very poor (the formula leads to a large over-estimate of the damping coefficient), a very good prediction of the experimental results was obtained by using equation (12). The numerical and analytical procedure here developed is then very adequate for the design of the device and the prediction of its characteristics.

REFERENCES

1. Poubeau, P.C.. October 1977. "High Speed Flywheels Operating on "One Active Axis" Magnetic Bearings", in 1977 Flywheel Technology Symposium, San Francisco, California, USA, pp.229-240.

2. Poubeau, P.C.. October 1980. "Flywheel Energy Storage Systems Operating on Magnetic Bearings", in 1980 Flywheel Technology Symposium, Scottsdale, Arizona, USA, pp.55-67.

3. Den Hartog, J. P.. 1947. Mechanical Vibrations, 3rd ed. McGraw Hill, New York, USA.

4. Genta, G., L. Mazzocchetti, and E. Rava. July 1990. "Magnetic Suspension for a Turbomolecular Pump", in Proceedings of the Second International Symposium on Magnetic Bearings, Tokio, Japan, pp.65-72.

5. Nikolajsen, J.L., R. Holmes, and V. Gondhalekar. 1979. "Investigation of an Electromagnetic Damper for Vibration Control of a Transmission Shaft", in Proceedings of the Institution of Mechanical Engineers, 193:331-336

6. Miki, M., Y. Tanaka, Y. Yamaguchi, T. Ishizawa, and A. Yamamura. July 1990. "Single Axis Active Magnetic Bearing System with Mechanical Dampers for High Speed Rotor", in Proceedings of the Second International Symposium on Magnetic Bearings, Tokio, Japan, pp.183-187.

7. Nagaya, K., and H. Koijma. 1984. "On a Magnetic Damper Consisting of a Circular Magnetic Flux and a Conductor of Arbitrary Shape. Part I: Derivation of the Damping Coefficients", Transactions of the ASME Journal of Dynamic Systems, Measurement and Control, 106(3):46-51.

8. Nagaya, K., and H. Koijma. 1984. "On a Magnetic Damper Consisting of a Circular Magnetic Flux and a Conductor of Arbitrary Shape. Part II: Applications and Numerical Results", Transactions of the ASME Journal of Dynamic Systems, Measurement and Control, 106(3):52-55.

9. Nagaya, K., H. Koijma, Y. Karube, and H. Kibayashi. 1984. "Braking Forces and Damping Coefficients of Eddy Current Brakes Consisting of Cylindrical Magnets and Plate Conductors of Arbitrary Shape", IEEE Transactions on Magnetic, MAG-20(6):2136-2145.

10. Nagaya, K., and Y. Karube. 1989. "A Rotary Magnetic Damper or Brake Consisting of a Number of Sector Magnets and a Circular Conductor", Transactions of the ASME Journal of Dynamic Systems, Measurement and Control, 111(3):97-104.

11. Nikolajsen, J.L.. 1988. "Experimental Investigation of an Eddy-Current Bearing", Magnetic Bearings, Springer, Berlin, pp.111-118.

12. Genta, G. Vibration of Structures and Machines, Springer, New York, U.S.A., to be published.

ACKNOWLEDGEMENTS

The present study was partially supported by Italian Ministry of University and Scientific Research under the 60% and 40% research grants.